Hydraulic disruption and passive migration by a bacterial pathogen in oak tree xylem

Article *in* Journal of Experimental Botany · February 2008

DOI: 10.1093/jxb/ern124 · Source: PubMed

3 authors, including:

Andrew Mcelrone
United States Department of Agriculture
80 PUBLICATIONS **2,164** CITATIONS

SEE PROFILE

Susan Jackson
Saint Joseph's University (PA, USA)
1 PUBLICATION **18** CITATIONS

SEE PROFILE

Journal of Experimental Botany, Vol. 59, No. 10, pp. 2649–2657, 2008
doi:10.1093/jxb/ern124 Advance Access publication 17 May, 2008
This paper is available online free of all access charges (see http://jxb.oxfordjournals.org/open_access.html for further details)

Journal of Experimental Botany
www.jxb.oxfordjournals.org

RESEARCH PAPER

Hydraulic disruption and passive migration by a bacterial pathogen in oak tree xylem

Andrew J. McElrone[1,*], Susan Jackson[2] and Piotr Habdas[3]

[1] *USDA-ARS Crops Pathology and Genetics Research Unit, University of California, Davis, CA 95616, USA*

[2] *Department of Biology, Saint Joseph's University, Philadelphia, PA 19131, USA*

[3] *Department of Physics, Saint Joseph's University, Philadelphia, PA 19131, USA*

Received 18 December 2007; Revised 4 April 2008; Accepted 7 April 2008

Abstract

***Xylella fastidiosa* (*Xf*) is a xylem-limited bacterial pathogen that causes leaf scorch symptoms in numerous plant species in urban, agricultural, and natural ecosystems worldwide. The exact mechanism of hydraulic disruption and systemic colonization of xylem by *Xf* remains elusive across all host plants. To understand both processes better, the functional and structural characteristics of xylem in different organs of both healthy and *Xf*-infected trees of several *Quercus* species were studied. Hydraulic conductivity (K_s) in *Xf*-infected petioles of *Q. palustris* and *Q. rubra* decreased significantly compared with healthy trees as the season progressed and plummeted to zero with the onset of scorch symptoms. Prior to the onset of symptoms, embolism was as much as 3.7 times higher in *Xf*-infected petioles compared with healthy controls and preceded significant reductions in K_s. Embolism likely resulted from pit membrane degradation during colonization of new petiole xylem and triggered the process that eventually led to vessel occlusion. Pit membrane porosity was studied using the following four methods to determine if a pathway exists in the xylem network of woody stems that allows for passive *Xf* migration: (i) calculations based on vulnerability to cavitation data, (ii) scanning electron micrographs, (iii) microsphere injections, and (iv) air seeding thresholds on individual vessels. All four methods consistently demonstrated that large pit membrane pores (i.e. greater than the diameter of individual *Xf*) occur frequently throughout the secondary stem xylem in several *Quercus* species. These large pores probably facilitate systemic colonization of the secondary xylem network and contribute to the high susceptibility to bacterial leaf scorch exhibited among these species.**

Key words: Cavitation, embolism, hydraulic conductivity, vascular pathogens, *Xylella fastidiosa*, xylem-limited bacteria.

Introduction

Xylella fastidiosa (Wells *et al*., 1987) is a xylem-limited bacterial pathogen that has a diverse host range and is the causal agent of numerous scorching, scalding, and stunting diseases worldwide (Hopkins and Purcell, 2002; Sherald and Kostka, 1992). Economically important diseases caused by *X. fastidiosa* (*Xf*) include citrus variegated chlorosis (CVC), Pierce's Disease of grape (PD), phony peach disease, alfalfa dwarf, periwinkle wilt, and bacterial leaf scorch of coffee, plum, pear, almond, mulberry, elm, oak, sycamore, maple, oleander, and pecan (Hopkins and Purcell, 2002). Bacterial leaf scorch (BLS) of shade trees has reached epidemic proportions in many urban and woodlot ecosystems throughout the eastern half of the United States. Surveys reveal that disease incidence can often exceed 50% in stands of mature shade trees throughout much of the geographic range (Frecon, 2002; Gould *et al*., 2004, 2007). Epidemics rivalling and exceeding BLS of shade trees are common to agricultural *Xf*-pathosystems. This is illustrated well in Brazilian citrus orchards where >120 million orange trees are currently affected by CVC (Hopkins and Purcell, 2002).

Evidence suggests that vascular wilt diseases targeting the xylem induce water stress in their hosts by increasing resistance to water flow (Tyree and Zimmerman, 2002). Historically, hydraulic dysfunction in diseases caused by

* To whom correspondence should be addressed. E-mail: ajmcelrone@ucdavis.edu

Xf has been attributed to host production of gels, gums, and tyloses and/or the accumulation of bacterial polysaccharides and cell masses that physically clog the vessels (reviewed by Hopkins, 1989). Currently, physical clogging induced by the bacteria themselves is the mechanism most widely accepted by researchers studying *Xf* pathosystems (Newman *et al*., 2003). Physical clogging undoubtedly plays an important role in symptom development particularly late in the growing season, however, the progression of events that lead from initial colonization of vessels to vascular occlusion late in the season are still not clearly understood.

Research with other vascular wilt pathogens has found that xylem-limited micro-organisms can initially reduce hydraulic flow by embolizing vessels. In both the Dutch elm and pine wilt pathosystems, embolism was found to precede vessel occlusion by the pathogens and contributed significantly to reductions in hydraulic conductivity (Newbanks *et al*., 1983; Ikeda and Kiyohara, 1995). McElrone *et al*. (2003) found no differences in embolism between healthy and *Xf*-infected Virginia creeper vines. However, measurements in this study ignored petioles, where much of the *Xf*-induced hydraulic dysfunction occurs in woody hosts (Hopkins, 1981). Additionally, the measurements were conducted only at the beginning and end of the growing season, thus the tissues and times where and when bacteria may induce embolism were potentially overlooked (McElrone *et al*., 2003). When the bacteria first enter a newly colonized conduit, they could cause emboli formation by lowering the surface tension of the water or by disturbing the pit membranes between adjacent vessels (Tyree and Sperry, 1989). Genomic and functional studies have shown that *Xf* possess cell wall-degrading enzymes that play a role in intervessel migration via pit membrane degradation (Simpson *et al*., 2000; Roper *et al*., 2007), which would possibly embolize the vessel prior to mass colonization and complete occlusion (Tyree and Zimmermann, 2002). Indeed, magnetic resonance imaging of small potted grapevines affected by Pierce's disease suggested that embolism formation and ethylene production are involved in the early stages of the infection process (Pérez-Donoso *et al*., 2006), but this pattern has yet to be investigated in other *Xf* host species especially for mature, field-grown plants.

Long-distance, systemic colonization of the host plant xylem network requires that *Xf* bacteria move efficiently across pit membranes between adjacent vessels. This would be especially true over the extensive vascular path lengths found in mature shade tree hosts. Even though *Xf* possess functional cell wall-degrading enzymes the systemic colonization would be eased in vascular systems with some continuous open pathways between vessels. McElrone *et al*. (2003) first suggested the existence of pit membrane pores large enough for *Xf* bacteria to migrate passively between vessels without the need for cell wall degradation. Pit membrane pore diameters as large as 0.3–0.4 μm have previously been measured in alfalfa (Van Alfen *et al*., 1983) and sugar maple (Sperry and Tyree, 1988), both of which are known hosts of *Xf* (Goheen *et al*., 1973; Hartman *et al*., 1996). Typical cellular dimensions for strains of *Xf* growing in culture are 0.25–0.35 by 0.9–3.5 μm (Wells *et al*., 1987). The majority of the pit membrane pores are narrower than a typical bacterium, but the presence of a few large pores may provide an opening large enough to accommodate a polarly oriented colonist bacterium. A high proportion (~80%) of vessels in PD-infected grapevines are often not blocked and contain solitary *Xf* cells possibly resulting from the successful long-distance movement of colonist bacteria through open pathways in woody tissue xylem (Newman *et al*., 2003; Gambetta *et al*., 2007). Host plant susceptibility and the speed with which *Xf* move systemically may be related to the size and frequency of large pit membrane pores across plant species (Chatelet *et al*., 2006; Thorne *et al*., 2006).

Understanding the exact mechanisms that contribute to hydraulic disruption, symptom development, and systemic colonization of host xylem will provide much-needed insight into the basis of structural host resistance. Specific objectives of the current study include: (i) documenting the extent of *Xf* infection in *Quercus* trees on an urban university campus in Philadelphia, PA; (ii) determining whether embolism is involved in the early in stages of hydraulic disruption and *Xf* colonization of new xylem of *Quercus* petioles; and (iii) determining whether large pores exist in the secondary xylem of woody stems that would facilitate long-distance passive movement of *Xf* in host tree xylem.

Materials and methods

ELISA testing

In October 2005 and 2006, several trees of four oak species were tested for *Xf*-infection using a double-antibody sandwich enzyme-linked immunosorbent assay (DAS-ELISA, AgDia, Inc., Elkhart, Indiana, USA). All the trees surveyed were growing as mature landscape trees on the Saint Joseph's University (SJU) campus in Philadelphia, PA. During the more extensive survey in October 2006, 66 total trees were tested from *Quercus rubra* L. (Northern Red Oak), *Quercus palustris* Muench. (Pin Oak), *Quercus alba* L. (Eastern White Oak), and *Quercus velutina* Lam. (Eastern Black Oak) (Table 1). The DAS-ELISA test system uses a mixture of antibodies from three serologically distinct isolates and detects a large panel of *Xf* isolates, including those from oak (Sherald and Lei, 1991). The samples were prepared as recommended by the manufacturer and briefly described here. Approximately 1 g of leaf tissue from each tree was combined with 10 ml of general extraction buffer and ground with a sterile mortar and pestle. One hundred μl of each pulverized tissue/buffer solution was transferred to an *Xf* antibody-coated well and incubated overnight in a refrigerated humid box. The wells were then carefully washed five times in phosphate-buffered saline Tween-20 solution (PBST) and

combined with 100 µl of peroxidase-conjugated antibody. After a second 2 h room temperature incubation in a humid box, each well was rewashed five times with PBST, combined with 100 µl of TMB peroxidase substrate solution, and incubated for 20 min at room temperature in a humid box. Each well was visually inspected for the blue colorimetric positive result for the presence of the bacteria. Wells containing separate positive and negative controls were included during all assays.

Leaf petiole hydraulic conductivity and per cent embolism

In each year of the study, trees used for physiological measurements were confirmed as healthy (control) and *Xf*-infected through visual inspection and ELISA testing as described above. Digital images of infected tree canopies taken at the end of the 2005 and 2006 growing seasons were used to ensure that leaves used for physiological measurements were located in symptomatic portions of the canopy in 2006 and 2007, respectively. Portions of the canopy that exhibited scorching in one year always exhibited symptoms in the subsequent year. Measurements commenced in the spring of each sampling season by pruning small branches containing several fully expanded leaves from several mature control and infected *Q. palustris* and *Q. rubra* trees. The excised branches and attached leaves were immediately sealed in plastic bags and brought to the laboratory for conductivity measurements. In the laboratory, the branches were submerged in a water bath and leaves were excised underwater. A hard plastic collar was then placed around the petiole and filled with dental epoxy resin to solidify/strengthen the tissue for clamping during hydraulic measurements (see McElrone *et al*., 2007, for more details of soft tissue preparation for hydraulic measurements). All leaf area distal to the collar was removed so that measurements were conducted on the petiole xylem only, and petiole lengths ranged from ~ 20–60 mm. All conductivity and embolism measurements were conducted on sun-exposed leaves under clear skies at midday throughout 2006 and 2007.

Two ultra-low flowmeters (ULFM) were constructed according to Tyree *et al*. (2002) to measure flow rates through the collared petioles. The ULFM measures the pressure drop (*dP*) across a standard PEEK capillary tube (diameter 0.13–0.18 mm, Upchurch Scientific, Oak Harbor, WA, USA) which has been calibrated to quantify the linear relationship between flow rate and *dP* (Tyree *et al*., 2002). Water flows through the ULFM via two Omnifit 8-way manifolds (U-06473-12, Cole-Parmer, Vernon Hills, IL, USA) with flow between the manifolds occurring through varying size PEEK tubing. *dP* between manifolds was measured by a differential pressure transducer (PX26, Omega, Stamford, CT, USA) and recorded every 2 s using a datalogger (CR10X, Campbell Scientific, Logan, UT, USA). Once flow was determined using the ULFM, specific hydraulic conductivity (K_s, kg s^{-1} MPa^{-1} m^{-1}) was calculated using the following equation:

$$K_s = ((Q_v/P)/A) \times L$$

where Q_v is the volumetric flow rate (kg s^{-1}), P (MPa) is the pressure applied to the ULFM, A (m^2) is the petiole cross-sectional area, and L (m) is the petiole length. After native K_s was measured at ⩽10 kPa for each petiole, a high pressure flush (⩾80 kPa) was used to remove any embolism from the petiole xylem. Post-flush final K_s was then taken at ⩽10 kPa, and the per cent embolism was calculated from the native and final K_s using the following equation

$$1-(K_s \text{ native}/K_s \text{ final}) \times 100$$

Distilled water was used for all K_s measurements and petiole flushing. Per cent embolism could not be measured on infected petioles when K_s reached zero.

Vulnerability curve calculations

Vulnerability to cavitation curves for stems of eight oak species were generated by Maherali *et al*. (2006) using the air-injection technique. These curves analyse the response of hydraulic conductivity of a given plant segment to increasing xylem tension. Maherali *et al*. (2006) provided us with the vulnerability curve data in order to derive the xylem tension required to reduce stem hydraulic conductivity by 25% (Ψ_{25}; i.e. xylem tension required to induce embolism in vessels that account for 25% of total stem flow). The curves for all eight species showed rapid increases in embolism with small increases in xylem tension. The Ψ_{25} values were used to calculate the pit membrane pore diameter with the following capillary equation as modified according to Sperry and Tyree (1988):

$$D = 4 \times (ST/\Delta P)$$

where D is the pit membrane pore diameter (µm), ST is the surface tension of the water at 25 °C (0.072 N m^{-1}), and ΔP is the air-seeding pressure gradient across the pit membrane (N m^{-2}; 1 MPa = 10^6 N m^{-2}). Ψ_{25} was substituted for ΔP in these calculations as it represents the pressure gradient required to pull an air-seed across a pit membrane pore between adjacent vessels (i.e. air-seeding threshold). All eight oak species are known symptomatic hosts of *Xf* (see data summary in Table 2).

Table 1. *ELISA test results for* Xylella fastidiosa*-infection in four oak species located on the Saint Joseph's University campus in summer 2006*

Oak species	Common name	No. trees tested	% Infected
Quercus rubra	Northern Red Oak	41	39.0
Quercus palustris	Pin Oak	21	47.6
Quercus alba	Eastern White Oak	3	33.3
Quercus velutina	Eastern Black Oak	1	0
		Total	**41%**

Table 2. *Pit membrane pore diameters calculated for seven oak species using the capillary equation*

Ψ_{25} values were extracted from cavitation vulnerability curve data generated on stems using the centrifuge technique by Maherali *et al*. (2006). All seven oak species listed in this table are known symptomatic hosts of *X. fastidiosa*. Capillary equation: $P = 4 \times (ST/D)$, where P is the pressure gradient across the pit membrane (N m^{-2}; 1 MPa = 10^6 N m^{-2}), ST is the surface tension of the water at 25 °C (0.072 N m^{-1}), D is the pore diameter (Tyree and Zimmermann, 2002). *X. fastidiosa* culture dimensions: 0.25–0.35 µm diameter×4.0 µm length (Wells *et al*., 1987).

Oak species	Common name	Ψ_{25} (MPa)	Calculated pit membrane pore diameter (µm)
Quercus alba	Eastern White Oak	0.586	0.491
Quercus falcata	Southern Red Oak	0.417	0.690
Quercus laevis	Turkey Oak	0.764	0.377
Quercus nigra	Water Oak	0.506	0.569
Quercus phellos	Willow Oak	0.711	0.405
Quercus rubra	Northern Red Oak	0.616	0.468
Quercus stellata	Post Oak	0.842	0.342

Environmental scanning electron microscopy (ESEM)

Stem samples from *Q. alba*, *Q. nigra*, and *Q. phellos* excised from mature landscape trees on the Duke University campus in April 2003 were immediately bagged and transported to the Biological Sciences SEM Facility at Duke University for imaging analysis. Segments of the woody tissue containing large xylem vessels from the newest annual ring were excised with a razor blade, pin-mounted with double-sided tape, and imaged immediately using a Philips XL 30 Environmental Scanning Electron Microscope (ESEM). The rapid sample preparation and lack of sample dehydration allows for examination of the pit membranes in a state as close as possible to native.

Microsphere injections

Polystyrene microspheres were perfused through hydrated stem segments of *Q. phellos, Q. alba*, and *Q. rubra* to estimate pit membrane pore size using two methods. Stem segments used in both methods were longer than the longest vessel for each species (verified by injecting stems with air at pressure below 5 kPa) and were perfused with degassed distilled water at high pressure (≥100 kPa) for ~30 min to remove all embolism and ensure full hydration of the sample. For the first injection method, an initial post-flush maximum K_s was measured with a low pressure head (≤10 kPa) prior to microsphere injection. Two sizes classes of the certified microspheres, 0.3 μm and 0.5 μm mean diameter (Duke Scientific Corporation, Palo Alto, CA; part numbers: 3300A and 3500A), were sequentially injected into the tubing upstream of the *Q. phellos* and *Q. alba* stems. K_s was remeasured as above after each successive microsphere injection. Spheres equal in size to the pit membrane pore diameters theoretically reduce K_s by wedging themselves into the pore and forming a tight seal, while those that have diameters smaller or larger than the pores either pass through or leave the pores unobstructed, respectively (see details in Jarbeau *et al*., 1995). For the second method, injected solution (0.3 μm spheres only) was collected from the downstream end of *Q. rubra* stems and examined for the presence of microspheres using bright field microscopy (Nikon TE-2000U microscope) and a video acquisition system. Using stems segments longer than the longest vessel ensured that spheres needed to cross pit membranes to exit the downstream end of the segment.

Air-seeding thresholds of individual vessels

Air-seeding thresholds were measured on individual earlywood vessels of *Q. palustris* and *Q. rubra* stem segments following a capillary insertion procedure similar to Choat *et al.* (2005) and Zwieniecki *et al.* (2001). Stem segments (~30 cm long) were pruned from asymptomatic branches on healthy trees of both species, placed immediately in plastic bags and transported to the laboratory for measurements. Segments of collected stems were cut down to ~3–6 cm length and the open ends were shaved with a new razor blade. Capillary tubes similar in diameter to the study vessels were pulled with pipette pullers (Sutter Instruments, Novato, CA and Model 51210, Stoelting Co. Wood Dale, IL), held in either a plastic collar by dental epoxy resin or a pipette holder (PM10, Stoelting Co, Wood Dale, IL, USA), and inserted by hand or with a micromanipulator with the aid of a stereomicroscope. Once inserted into an individual vessel, the needles were held in the vessel and strengthened by cyanoacrylate glue and an accelerator (Loctite 401 and 712, Henkle Corp., Rocky Hill, CT, USA) to close all of the open vessels on one side of the segment. A dilute safranin dye solution (0.01% w/v) was then forced through the individual vessel to identify its open-end on the distal end of the stem. The open-end of the dyed vessel was carefully glued using a capillary tube as an applicator. This procedure required injected air to travel laterally to adjacent vessels via intervessel pit membranes. The needle was then attached to a pressurized nitrogen tank or pressure chamber (Model 600, Plant Moisture Systems, Corvallis, OR, USA) and the open end of the distal end of the stem was placed into a beaker of water. Air pressure was increased slowly until bubbles appeared exiting a vessel adjacent to the glued one at the distal submerged end of the stem. Air pressures required to induce the bubble stream were used to calculate pit membrane pore sizes for each species by using the capillary equation as described above (data are presented as pit membrane pore calculations in Fig. 5). This procedure was conducted on both new earlywood vessels (located in the outermost annual ring) as well as older earlywood vessels (annual rings ≥3 years old) in similar stem segments.

Statistical analysis

Analysis of variance was performed on the seasonal K_s and per cent embolism data using SPSS 12.0 (SPSS, Chicago, IL) to test for main affects of infections status. Means separation tests were utilized to resolve significant differences on individual dates.

Results

A large percentage (41%) of all the oak trees sampled on the SJU campus tested positive for *Xf* infection (Table 1) and exhibited various stages of leaf scorch and branch dieback symptoms throughout their canopies. This severe level of disease incidence is consistent with that of other landscaped plantings in the surrounding area. *Q. rubra* and *Q. palustris* comprised the vast majority of trees growing on the SJU campus, and these species exhibited 39% and 48% disease incidence, respectively (Table 1). Many of the infected trees with extensive canopy dieback were very large specimens (>100 years old). All trees used for the physiological measurements remained in their respective infection status throughout the study (i.e. control trees never exhibited leaf scorch symptoms and always tested negative for *Xf*), and infected trees showed symptoms consistently in the same portions of the canopy from year to year.

Petiole K_s for both species was similar between control and *Xf*-infected trees at the beginning of both growing seasons ($P > 0.05$) but diverged with the onset of leaf scorch symptoms (Figs 1, 2). This divergence was driven mainly by a decrease in *Xf*-infected petioles while K_s of control petioles remained relatively constant throughout the measurement period in both seasons. K_s of infected petioles eventually plummeted to zero by mid to late summer. The decrease in K_s occurred gradually for *Q. palustris*-infected petioles (Fig. 1B) while the decrease was more abrupt in *Q. rubra* (Fig. 2A, B). Water soaking and initial scorching of the leaf margin began as K_s began to drop, but severe scorching and development of the chlorotic halo only became apparent when K_s approached zero.

The percentage embolism in petioles was also similar at the beginning of the growing season (illustrated well in Fig. 1D), but exhibited different patterns between control

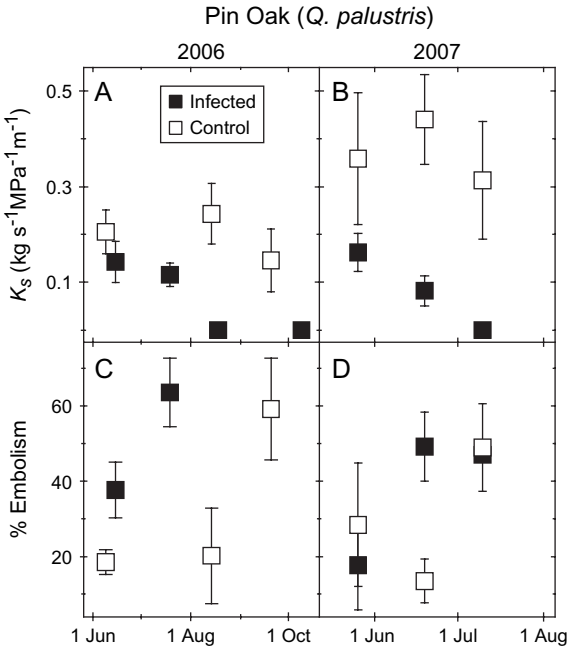

Fig. 1. Specific hydraulic conductivity (K_s) (A, B) and per cent embolism (C, D) measured on *Q. palustris* petioles throughout both 2006 (left panels) and 2007 (right panels) growing seasons. *X. fastidiosa*-infection status of all trees was verified using ELISA from 2005–2007. All study trees were located on the Saint Joseph's University campus in Philadelphia, PA. Per cent embolism could not be measured on infected petioles when K_s reached zero. Data points represent the mean ±SE of n=4–8 petioles.

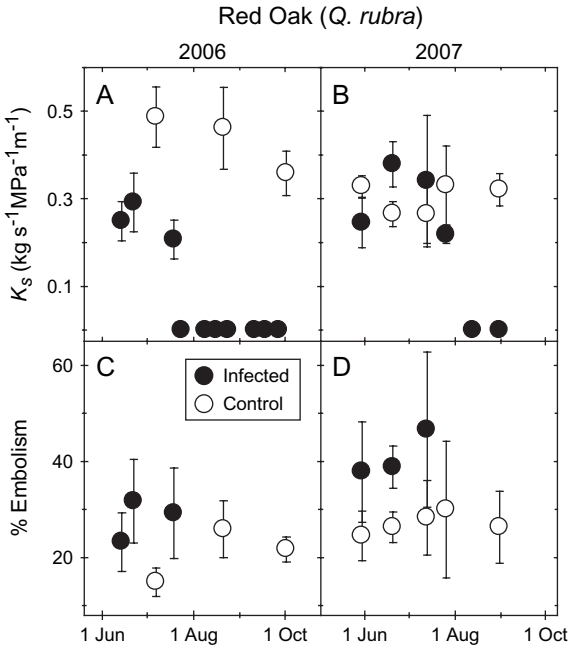

Fig. 2. Specific hydraulic conductivity (A, B) and per cent embolism (C, D) measured on *Q. rubra* petioles throughout both 2006 (left panels) and 2007 (right panels) growing seasons. *X. fastidiosa*-infection status of all trees was verified using ELISA from 2005–2007. All study trees were located on the Saint Joseph's University campus in Philadelphia, PA. Data points represent the mean ±SE of n=4–8 petioles.

and *Xf*-infection as the season progressed. Embolism in *Xf*-infected petioles increased prior to that of control petioles particularly in *Q. palustris* and was as much as 3.7 times greater in June 2007 (P=0.03) (Fig. 1C, D). In general, increased embolism also preceded any significant decrease in K_s. Eventually both control and infected petioles reached similar levels of embolism late in the season ($P > 0.05$) (Fig. 1C, D). Even though percentage embolism reached a similar level in both control and infected *Q. palustris* petioles by the end of the growing season, the K_s remained significantly greater in control trees. This suggests that the K_s decrease in *Xf*-infected petioles are initiated by embolism but require vessel occlusion by additional means to induce massive hydraulic failure. A similar pattern of increased embolism was illustrated in *Q. rubra*-infected petioles, but this increase was maintained throughout the growing seasons (Fig. 2D; P=0.037).

Four varying techniques were used to demonstrate directly and indirectly the presence of pores in secondary xylem pit membranes that are larger than the mean diameter of a bacterium. Vulnerability curve data collected previously by Maherali *et al.* (2006) consistently demonstrated that low air-seeding pressures were needed to induce substantial embolism in stems of all seven oak species; the mean Ψ_{25} was 0.635 MPa across the species. Calculated pore diameters ranged from 0.342 to 0.690 μm across the species and thus were always larger than the mean diameter of *Xf* (0.30 μm) (Table 2). ESEM images demonstrated that the large pores predicted from the vulnerability curve data are present in the intervessel pit membranes of *Q. alba*, *Q. phellos*, and *Q. nigra* (Fig. 3). Pit membranes were found in various conditions from fully intact (i.e. no large pores) (Fig. 3A, B) to those containing pores >1.0 μm (Fig. 3B). The presence of intact pit membranes suggests that ESEM analysis of fresh tissue is effective at limiting damage caused by sample dehydration necessary for other electron microscopic techniques. Reductions of woody stem K_s induced by microsphere injections also consistently demonstrated the presence of pores as large as the diameter of a *Xf* bacterium, particularly in *Q. phellos* (Fig. 4). Microspheres were able to pass the entire distance of *Q. rubra* stem segments longer than the longest vessel (verified with air injection at low pressure) (data not shown).

Air-seeding thresholds were measured on individual earlywood vessels from the current and older growth rings to verify that these pores are present across all of the secondary xylem. Vulnerability curves and microsphere injection techniques integrate all vessels and do not distinguish between vessels of varying age. Based on air-seeding threshold pressures of individual vessels, large pit membrane pores were commonly found (>40% frequency for all vessel classes) in current and older earlywood vessels of both *Q. rubra* and *Q. palustris* (Fig. 5).

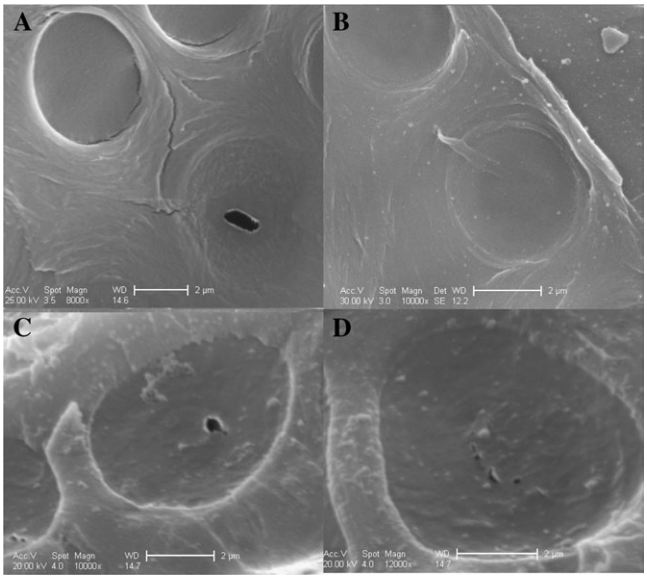

Fig. 3. ESEMs of *Quercus nigra* (A), *Q. phellos* (B), and *Q. alba* (C, D) pit membranes between adjacent secondary xylem vessels in stems. Large pit membrane pores were found in all species and ranged in size from 0.16–0.85 μm across the species. Images show various pit membranes ranging from intact (i.e. no large pores) (A, B) to those with very large perforations (B, C). Images were taken at the Duke University, Biological Sciences SEM facility in Durham, NC.

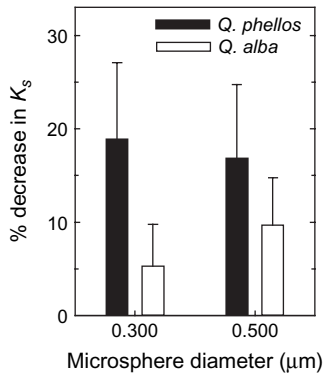

Fig. 4. Percentage decrease in hydraulic conductivity of *Q. phellos* and *Q. alba* stems injected with microspheres of varying mean diameter. Microsphere injection reduces conductivity by sealing pit membrane pores equal in diameter to the spheres (see Materials and methods for details).

Discussion

These results demonstrate that embolism is an integral component of *Xf* pathogenesis and is involved in the early colonization of petiole xylem prior to the onset of leaf scorch symptoms in mature oaks. Recent magnetic resonance imaging of small potted grapevines showed that PD infection caused embolism in stems prior to symptom development in the leaves (Pérez-Donoso *et al*., 2006). A similar sequence is induced by fungal and nematode vascular pathogens in the Dutch elm and Pine wilt

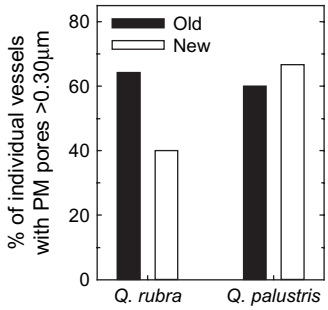

Fig. 5. Percentage of single vessels containing pit membrane pores >0.30 μm for *Q. rubra* and *Q. palustris*. Pit membrane pore sizes were determined using air-seeding threshold pressures and the capillary equation (see equation and single-vessel measurement details in the Materials and methods). Single large earlywood vessels were characterized as new (from the outermost annual growth ring) or old (from ⩾3rd annual growth ring). Data bars represent the means of n=13–15 for each vessel category within a given species.

pathosystems, respectively (Newbanks *et al*., 1983; Ikeda and Kiyohara, 1995). McElrone *et al*. (2003) found no increased embolism in *Xf*-infected Virginia creeper vines, but measurements in this study were limited to woody stems and to the beginning and end of the growing season, probably missing where and when the bacteria induce embolism. Measurements of leaf petioles are more likely to reveal the importance of embolism to pathogenesis since visual symptoms and much of the hydraulic dysfunction caused by *Xf* occur in the leaves and petioles of woody hosts (Hopkins, 1981). This may be especially important given that xylem anatomy can differ between organs within a given host plant (see details below).

Vascular occlusion induced by *Xf*-infection has been largely attributed to clogging by the bacteria themselves and the polysaccharide gels they produce (Hopkins, 1989; Krivanek and Walker, 2005; Newman *et al*., 2003). Our current data in combination with other recent studies, suggest that *Xf*-pathogenesis follows a more complicated sequence, probably starting with the embolism of vessels. Embolism was detected in *Xf*-infected *Q. rubra* and *Q. palustris* prior to a substantial decrease in petiole K_s, which suggests that embolism formation intitiates the hydraulic disruption, but is not entirely responsible for occlusion. Gambetta *et al*. (2007) used a highly sensitive detection technique to show that PD leaf scorch symptoms can form even in the absence of localized high concentrations of the bacteria and suggested that plant hormones may regulate such a systemic response. The hormone ethylene was recently shown to induce both emboli and tyloses formation in grapevines (Pérez-Donoso *et al*., 2006; Sun *et al*., 2006) and to be produced in greater concentrations in leaves of PD-infected grapevines (Pérez-Donoso *et al*., 2006). Tyloses are known to form in vessels of *Q. rubra* and *Q. alba* after irreversible embolism under natural, non-infected conditions (Cochard and Tyree, 1990) and form as a response to the loss of

vessel water in many species (Tyree and Zimmermann, 2002). Cochard and Tyree (1990) stated that the presence of air embolism in *Quercus* vessels is an absolute requirement for subsequent growth of tyloses in a given conduit. More work is clearly needed to resolve the ultimate mechanism of occlusion and whether embolism leads to ethylene production and subsequent tylose formation and if this response is ubiquitous among *Xf* hosts.

When the bacteria first enter a newly colonized conduit, they may cause emboli formation by lowering the surface tension of the water (Ikeda and Kiyohara, 1995; Tyree and Sperry, 1989) or by disturbing the pit membranes between adjacent vessels (Sperry and Tyree, 1988). Recent genomic and functional analyses have shown that *Xf* possess polygalacturonases, cellulases, and other cell-wall degrading enzymes that are assumed to play a role in intervessel migration via pit membrane degradation throughout the entirety of a host's vasculature (Simpson *et al*., 2000; Roper *et al*., 2007). Many electron micrographs of petiole xylem from various shade tree hosts have shown large cell masses loaded into single vessels while surrounding vessels are free of bacteria (Hearon *et al*., 1980; see Fig. 6 within their publication; Gould and Lashomb, 2005; image of Pin oak by JR Hartman). The bacteria in these images are often loaded into pit chambers and pressed against the pit membrane, but only on the side of the mass colonized vessel. Recent work studying systemic movement in grapevines using *Xf* expressing green fluorescent protein has shown that the bacteria are very often found as solitary cells and less frequently as mass colonies packed into a single petiole vessel (Newman *et al*., 2003). The images in these studies suggest that the bacteria are inefficient at rapidly digesting pit membranes and often get caught in vessels that lack unobstructed open pathways to a neighbouring vessel. Efficient long-distance colonization of host vasculature may therefore require additional strategies to migrate systemically through host xylem.

Pit membrane characteristics and thus vulnerability to cavitation can vary dramatically between various organs within a given plant (McElrone *et al*., 2004; Choat *et al*., 2005). Petioles of some species are known to be more resistant to cavitation than their stems (Sperry and Saliendra, 1994; Hacke and Sauter, 1996). If this pattern holds for both *Q. rubra* and *Q. palustris*, the largest pit membrane pores of petiole vessels would be smaller than those in woody stems and roots and thus require cell wall degradation during colonization of this xylem tissue. Spatially variable *Xf* distributions within hosts as documented by Newman *et al*. (2003) are expected if the long-distance movement is dependent upon the frequency of open pathways within a xylem network (Chatelet *et al*., 2006). Just as water encounters higher resistance to flow when it crosses pit membranes relative to axial flow in the vessel lumen (Choat *et al*., 2006), intact pit membranes with minute pores would also act to limit the movement of *Xf* during systemic migration. McElrone *et al*. (2003) first suggested that the presence of large pit membrane pores would facilitate the passive migration of *Xf* throughout host vasculature. Using a suite of techniques in this study, we have consistently demonstrated the presence of pit membrane pores larger than single *Xf* cells for a range of oak species. Our findings are in agreement with the large pit membrane pores (>0.90 μm) measured via air-seeding thresholds in individual vessels from the current annual ring of *Q. rubra* stems (B Choat *et al*., personal communication). Similar work has recently shown that passive networks exist in grapevines that allow long-distance passive migration through host vasculature (Chatelet *et al*., 2006; Thorne *et al*., 2006). Ultimately, *Xf* resistance/tolerance [i.e. ability to limit systemic spread from an inoculation point (see Krivanek and Walker 2005)] of host plants and cultivars are probably driven by pit membrane structural characteristics such as resistance to enzymatic degradation and the frequency and size of abnormally large pit membrane pores.

Xylem vessels containing large pit membrane pores, such as those documented here for various *Quercus* species, would embolize under very low tension. For species that lack refilling and embolism repair mechanisms, such vessels may function for only a short period of time in the early spring (e.g. earlywood vessels; Cochard and Tyree, 1990) before becoming embolized. Movement through these vessels in the early spring may provide a sufficient low resistance pathway to allow rapid long-distance migration. Such a mechanism may explain why only early season (April–May) PD infections of grapevine persist and become chronic the following season (Feil *et al*., 2003).

The biological and economic impacts of *Xf* infection are clear across host plants in urban, agricultural, and natural ecosystems. BLS threatens numerous shade trees (including 18 *Quercus* species) from Florida to southern New England and west to Nebraska, and has reached epidemic proportions in many parts of its expanding geographic range (Gould *et al*., 2007). The small area of the SJU campus covered in our survey is representative of the problem facing much of the region, and the aesthetics of these areas will be drastically altered upon the eventual removal of these declining trees. Developing a thorough understanding of *Xf* pathogenesis across the full range of hosts will enable us to manage and breed plants to avoid the loss of these valuable resources.

Acknowledgements

The authors would like to thank J Bichler for assistance with the ULFM and oak BLS survey, H Maherali, C Moura, and R Jackson for providing us with the

vulnerability curve data, L Eibest for training and assistance with ESEM imaging at the Duke University Biological Science SEM Facility, R Addington, S Buch, A Krafnick, J Lee, B McPherson, F Palladino, K Pearsall, M Serio, and C Stone for various help with the microsphere injections, petiole conductivity, ESEM imaging, and single vessel measurements, the SJU facilities department for maintenance of BLS trees, and B Choat and K Steenwerth for helpful editorial comments on the manuscript. Funds from several grants were provided by the SJU Chapter of Sigma Xi.

References

Chatelet DS, Matthews MA, Rost TL. 2006. Xylem structure and connectivity in grapevine (*Vitis vinifera*) shoots provides a passive mechanism for the spread of bacteria in grape plants. *Annals of Botany* **98,** 483–494.

Choat B, Brodie TW, Cobb AR, Zwieniecki MA, Holbrook NM. 2006. Direct measurements of intervessel pit membrane hydraulic resistance in two angiosperm tree species. *American Journal of Botany* **93,** 993–1000.

Choat B, Lahr EC, Melcher PJ, Zwieniecki MA, Holbrook NM. 2005. The spatial pattern of air seeding thresholds in mature sugar maple trees. *Plant, Cell and Environment* **28,** 1082–1089.

Cochard H, Tyree MT. 1990. Xylem dysfunction in *Quercus*: vessel sizes, tyloses, cavitation and seasonal changes in embolism. *Tree Physiology* **6,** 393–407.

Feil H, Feil WS, Purcell AH. 2003. Effects of date of inoculation on the within-plant movement of *Xylella fastidiosa* and persistence of Pierce's Disease within field grapevine. *Phytopathology* **93,** 244–251.

Frecon JL. 2002. *Bacterial leaf scorch attacks New Jersey's oak trees*. Rutgers Cooperative Extension publication.

Gambetta GA, Fei J, Rost TL, Matthews MA. 2007. Leaf scorch symptoms are not correlated with bacterial populations during Pierce's disease. *Journal of Experimental Botany* **58,** 4037–4046.

Goheen AC, Nyland G, Lowe SK. 1973. Association of a rickettsia-like organism with Pierce's disease of grapevines and alfalfa dwarf and heat therapy of the disease in grapevines. *Phytopathology* **63,** 341–345.

Gould AB, Hamilton G, Vodak M, Grabosky J, Lashomb J. 2004. Bacterial leaf scorch of oak in New Jersey: incidence and economic impact. *Phytopathology* **94,** S36.

Gould AB, Hamilton G, Vodak M, Grabosky J, Staniszewska H, Lashomb J. 2007. Incidence and severity of bacterial leaf scorch of oak in New Jersey urban forest. *Phytopathology* **97,** S178.

Gould AB, Lashomb J. 2005. *Bacterial leaf scorch of shade trees*. APSnet Feature Story. November 2005. www.apsnet.org.

Hacke U, Sauter JJ. 1996. Drought-induced xylem dysfunction in petioles, branches, and roots of *Populus balsamifera* L. and *Alnus glutinosa* (L.) Gaertn. *Plant Physiology* **111,** 413–417.

Hartman JR, Jarlfors UE, Fountain WM, Thomas R. 1996. First report of bacterial leaf scorch caused by *Xylella fastidiosa* on sugar maple and sweetgum. *Plant Disease* **80,** 1302.

Hearon SS, Sherald JL, Kostka SJ. 1980. Association of xylem-limited bacteria with elm, sycamore, and oak leaf scorch. *Canadian Journal of Botany* **58,** 1986–1993.

Hopkins DL. 1989. *Xylella fastidiosa*: xylem-limited bacterial pathogens of plants. *Annual Review of Phytopathology* **27,** 271–290.

Hopkins DL. 1981. Seasonal concentration of the Pierce's disease bacterium in grapevine stems, petioles, and leaf veins. *Phytopathology* **71,** 415–418.

Hopkins DL, Purcell AH. 2002. *Xylella fastidiosa*: cause of Pierce's disease of grapevine and other emergent diseases. *Plant Disease* **86,** 1056–1066.

Jarbeau JA, Ewers FW, Davis SD. 1995. The mechanism of water-stress-induced embolism in two species of chaparral shrubs. *Plant, Cell and Environment* **18,** 189–196.

Krivanek AF, Walker MA. 2005. *Vitis* resistance to Pierce's disease is characterized by differential *Xylella fastidiosa* populations in stems and leaves. *Phytopathology* **95,** 44–52.

Ikeda T, Kiyohara T. 1995. Water relations, xylem embolism, and histological features of *Pinus thunbergii* inoculated with virulent or avirulent pine wood nematode, *Bursaphelenchus xylophilus*. *Journal of Experimental Botany* **46,** 441–449.

Maherali H, Moura CF, Caldeira MC, Willson CJ, Jackson RB. 2006. Functional coordination between leaf gas exchange and vulnerability to xylem cavitation in temperate forest trees. *Plant, Cell and Environment* **29,** 571–583.

McElrone AJ, Bichler J, Pockman WT, Addington RN, Linder CR, Jackson RB. 2007. Aquaporin-mediated changes in hydraulic conductivity of deep tree roots accessed via caves. *Plant, Cell and Environment* **30,** 1411–1421.

McElrone AJ, Pockman WT, Martinez-Vilalta J, Jackson RB. 2004. Variation in xylem structure and function in stems and roots of trees to 20 m depth. *New Phytologist* **163,** 507–517.

McElrone AJ, Sherald JL, Forseth IN. 2003. Interactive effects of water stress and xylem-limited bacterial infection on the water relations of a host vine. *Journal of Experimental Botany* **54,** 419–430.

Newbanks D, Bosch A, Zimmermann MH. 1983. Evidence for xylem dysfunction by embolism in Dutch Elm Disease. *Phytopathology* **73,** 1060–1063.

Newman KL, Almeida RPP, Purcell AH, Lindow SE. 2003. Use of a green fluorescent strain for analysis of *Xylella fastidiosa* colonization of *Vitis vinifera*. *Applied and Environmental Microbiology* **69,** 7319–7327.

Pérez-Donoso AG, Greve LC, Walton JH, Shackel KA, Labavitch JM. 2006. *Xylella fastidiosa* infection and ethylene exposure result in xylem and water movement disruption in grapevine shoots. *Plant Physiology* **143,** 1024–1036.

Roper MC, Greve LC, Warren JG, Labavitch JM, Kirkpatrick BC. 2007. *Xylella fastidiosa* requires polygalacturonase for colonization and pathogenicity in *Vitis vinifera* grapevines. *Molecular Plant–Microbe Interactions* **20,** 411–419.

Sherald JL, Kostka SJ. 1992. Bacterial leaf scorch of landscape trees caused by *Xylella fastidiosa*. *Journal of Arboriculture* **18,** 57–63.

Sherald JL, Lei JD. 1991. Evaluation of a rapid ELISA test kit for detection of *Xylella fastidiosa* in landscape trees. *Plant Disease* **75,** 200–203.

Simpson AJ, Reinach FC, Arruda P, *et al.* 2000. The genome sequence of the plant pathogen *Xylella fastidiosa*. *Nature* **406,** 151–157.

Sperry JS, Saliendra NZ. 1994. Intra- and inter-plant variation in xylem cavitation in *Betula occidentalis*. *Plant, Cell and Environment* **17,** 1233–1241.

Sperry JS, Tyree MT. 1988. Mechanism of water stress-induced xylem embolism. *Plant Physiology* **88,** 581–587.

Sun Q, Rost TL, Matthews MA. 2006. Pruning-induced tylose development in stems of current-y.ear shoots of *Vitis vinifera* (Vitaceae). *American Journal of Botany* **93,** 1567–1576.

Thorne E, Young BM, Young GM, Stevenson JF, Labavitch JM, Matthews MA, Rost TL. 2006. The structure of xylem vessels

in grapevine and a possible passive mechanism for the systemic spread of bacterial disease. *American Journal of Botany* **93,** 497–504.

Tyree MT, Sperry JS. 1989. Vulnerability of xylem to cavitation and embolism. *Annual Review of Plant Physiology and Molecular Biology* **40,** 19–38.

Tyree MT, Vargas G, Engelbrecht BMJ, Kursar TA. 2002. Drought until death do us part: a case study of the desiccation-tolerance of a tropical moist forest seedling-tree, *Licania platypus* (Hemsl.) Fritsch. *Journal of Experimental Botany* **53,** 2239–2247.

Tyree MT, Zimmermann MH. 2002. *Xylem structure and the ascent of sap*, 2nd edn. Berlin: Springer-Verlag.

Van Alfen NK, McMillan BD, Turner V, Hess WM. 1983. Role of pit membranes in macromolecule-induced wilt of plants. *Plant Physiology* **73,** 1020–1023.

Wells JM, Raju BC, Hung HY, Weisburg WG, Mandelco-Paul L, Brenner DJ. 1987. *Xylella fastidiosa*: gram-negative, xylem-limited, fastidious plant bacteria related to *Xanthomonas*. *International Journal of Systematic Bacteriology* **37,** 136–143.

Zwieniecki MA, Melcher P, Holbrook NM. 2001. Hydraulic properties of individual xylem vessels of *Fraxinus americana*. *Journal of Experimental Biology* **52,** 257–264.